







Earth's Future

RESEARCH ARTICLE

10.1029/2023EF004399

Forest Carbon Storage in the Western United States: Distribution, Drivers, and Trends

Jazlynn Hall¹ , Manette E. Sandor¹ , Brian J. Harvey² , Sean A. Parks³ ,
Anna T. Trugman⁴ , A. Park Williams⁵ , and Winslow D. Hansen¹ 

¹Cary Institute of Ecosystem Studies, Millbrook, NY, USA, ²School of Environmental and Forest Sciences, University of Washington, Seattle, WA, USA, ³Aldo Leopold Wilderness Research Institute, Rocky Mountain Research Station, USDA Forest Service, Missoula, MT, USA, ⁴Department of Geography, University of California Santa Barbara, Santa Barbara, CA, USA, ⁵Department of Geography, University of California Los Angeles, Los Angeles, CA, USA

Key Points:

- Live carbon has declined across much of western United States forests, likely due to drought and fire, resulting in an increase in dead carbon
- In the Pacific Northwest (PNW), harvest led to reduced carbon, but recovery from past harvest likely caused carbon to increase since 2005
- Our results provide a baseline from which to evaluate future changes and inform management strategies

Supporting Information:

Supporting Information may be found in the online version of this article.

Correspondence to:

J. Hall,
hallj@caryinstitute.org

Citation:

Hall, J., Sandor, M. E., Harvey, B. J., Parks, S. A., Trugman, A. T., Williams, A. P., & Hansen, W. D. (2024). Forest carbon storage in the western United States: Distribution, drivers, and trends. *Earth's Future*, 12, e2023EF004399. <https://doi.org/10.1029/2023EF004399>

Received 22 DEC 2023

Accepted 29 APR 2024

Author Contributions:

Conceptualization: Jazlynn Hall, Manette E. Sandor, Anna T. Trugman,

A. Park Williams, Winslow D. Hansen

Data curation: Jazlynn Hall, Sean A. Parks

Formal analysis: Jazlynn Hall, Sean A. Parks, Anna T. Trugman, A. Park Williams

Funding acquisition: Winslow D. Hansen

Investigation: Jazlynn Hall, Winslow D. Hansen

Methodology: Jazlynn Hall, Manette E. Sandor, Sean A. Parks, Anna

Abstract Forests are a large carbon sink and could serve as natural climate solutions that help moderate future warming. Thus, establishing forest carbon baselines is essential for tracking climate-mitigation targets. Western US forests are natural climate solution hotspots but are profoundly threatened by drought and altered disturbance regimes. How these factors shape spatial patterns of carbon storage and carbon change over time is poorly resolved. Here, we estimate live and dead forest carbon density in 19 forested western US ecoregions with national inventory data (2005–2019) to determine: (a) current carbon distributions, (b) underpinning drivers, and (c) recent trends. Potential drivers of current carbon included harvest, wildfire, insect and disease, topography, and climate. Using random forests, we evaluated driver importance and relationships with current live and dead carbon within ecoregions. We assessed trends using linear models. Pacific Northwest (PNW) and Southwest (SW) ecoregions were most and least carbon dense, respectively. Climate was an important carbon driver in the SW and Lower Rockies. Fire reduced live and increased dead carbon, and was most important in the Upper Rockies and California. No ecoregion was unaffected by fire. Harvest and private ownership reduced carbon, particularly in the PNW. Since 2005, live carbon declined across much of the western US, likely from drought and fire. Carbon has increased in PNW ecoregions, likely recovering from past harvest, but recent record fire years may alter trajectories. Our results provide insight into western US forest carbon function and future vulnerabilities, which is vital for effective climate change mitigation strategies.

Plain Language Summary We investigated the role of western US forests as natural climate solutions by analyzing current forest carbon storage and trends from 2005 to 2019 across 19 forested regions. We found that the Pacific Northwest stores the most carbon, while the Southwest stores the least. Climate, wildfires, and human activities determined carbon amounts. For instance, climate is important in the Southwest and Lower Rockies, while wildfires impact the entire western US, but particularly the Upper Rockies and California. Human activities like harvesting and private ownership, decrease carbon, particularly in the Pacific Northwest. Since 2005, live carbon has declined in many western US areas, likely due to drought and fires. The study highlights the vulnerability of western US forests to climate-related and human threats to carbon, providing crucial insights for effective climate change mitigation strategies. Understanding these dynamics is essential for scientists, policymakers, and educators working toward sustainable forest management and climate solutions in the region.

1. Introduction

Determining how, where, and why forest carbon is shifting is a profound global challenge (DeFries et al., 2022). Forests play a crucial role in the global carbon cycle, contributing to over half of terrestrial carbon stocks (Friedlingstein et al., 2022; Harris et al., 2021) with large potential to store more carbon (Walker et al., 2022). Many climate mitigation pathways that successfully keep additional warming below 1.5°C this century rely in part on additional forest carbon storage (Rogelj et al., 2018). As a result, momentum is building to leverage forests as natural climate solutions, where ecosystems are actively managed to increase carbon storage or reduce emissions (Griscom et al., 2017; Hepburn et al., 2019; Rockström et al., 2021).

Natural climate solutions are currently fraught with issues such as greenwashing, lack of regulation, and accounting practices unmoored from credible carbon-cycle science (Novick et al., 2022). Such issues have resulted in poor understanding of current baselines and potential drivers of trajectories (Anderegg et al., 2020;

© 2024 The Author(s). Earth's Future published by Wiley Periodicals LLC on behalf of American Geophysical Union. This article has been contributed to by U.S. Government employees and their work is in the public domain in the USA.

This is an open access article under the terms of the [Creative Commons Attribution License](https://creativecommons.org/licenses/by/4.0/), which permits use, distribution and reproduction in any medium, provided the original work is properly cited.

T. Trugman, A. Park Williams, Winslow D. Hansen

Project administration: Winslow D. Hansen

Resources: Manette E. Sandor, Brian J. Harvey, Winslow D. Hansen

Software: Jazlynn Hall, Sean A. Parks

Supervision: Winslow D. Hansen

Validation: Jazlynn Hall, Manette E. Sandor, Brian J. Harvey, Sean A. Parks, Anna T. Trugman, A. Park Williams, Winslow D. Hansen

Visualization: Jazlynn Hall

Writing – original draft: Jazlynn Hall, Manette E. Sandor, Winslow D. Hansen

Writing – review & editing: Jazlynn Hall, Manette E. Sandor, Brian J. Harvey, Sean A. Parks, Anna T. Trugman, A. Park Williams, Winslow D. Hansen

Gifford, 2020). Specifically, the spatial distribution of current forest carbon, the factors that underpin patterns of forest carbon, and the associated drivers and trends are often poorly resolved, particularly at landscape to regional scales (Harris et al., 2021; Zhang et al., 2019). Thus, establishing rigorous baselines of current forest carbon storage is essential for tracking future progress toward climate-mitigation targets. Such baselines will enhance the rigor and transparency of policy and market mechanisms using these forests as natural climate solutions (Badgley et al., 2022).

Some estimates suggest that the terrestrial carbon sink has doubled since the 1960s (Ruehr et al., 2023). In tropical forests, this is driven by increased photosynthesis from elevated atmospheric CO₂ concentrations (Walker et al., 2021), while warming is increasing productivity in cold, high latitude forests (Keenan & Riley, 2018; Ruehr et al., 2023). Today, global forests sequester as much as 7.8 GtCO₂e yr⁻¹ (Harris et al., 2021), 60% of the total terrestrial carbon sink (Friedlingstein et al., 2022). However, future forest carbon storage will depend on avoiding emissions from deforestation and climate driven changes to disturbance regimes that can erode forest permanence and resilience (Anderegg et al., 2020).

Global drought trends are on the rise (Chiang et al., 2021; Spinoni et al., 2019), leading to diminished terrestrial water storage (Pokhrel et al., 2021), increased plant water stress (Trugman et al., 2020), and elevated tree mortality (Anderegg et al., 2020; Hammond et al., 2022). In many places, extreme droughts are amplifying the frequency, size and severity of climate-sensitive disturbances, like fire and insect outbreaks, that can cause widespread tree mortality and convert vast quantities of carbon from live to dead pools (Jones et al., 2022; Lehmann et al., 2020). Globally, fires currently account for 38% of forest cover loss (Hansen et al., 2013; van Wees et al., 2021) and cause emissions that counter the land carbon sink (Chen et al., 2023; Zheng et al., 2021). Together, climate change and climate-sensitive disturbances are almost certain to profoundly erode current forest carbon and future storage potential that could inhibit meaningful climate mitigation in coming decades (Anderegg et al., 2020; Anderegg, Wu, et al., 2022).

To successfully avoid additional emissions, it may be critical to prevent deforestation and severe disturbances in the boreal forest biome and arid temperate forests in particular (Tagesson et al., 2020; H. Yang et al., 2023). Temperate and boreal forests currently constitute two thirds of the net forest carbon sink (Harris et al., 2021), but numerous persistent and growing drivers can erode carbon storage. In the western US, human harvest plays an outsized role in forest landscapes, contributing up to 50% of tree mortality between 2003 and 2012 (Berner et al., 2017). The region appears to have recently emerged from the worst megadrought in 1200 years (Williams et al., 2022), and extreme drought risk in western North America is projected to increase by as much as 300% relative to a pre-industrial baseline by the end of the 21st century (Cook et al., 2020). Accompanying trends in drought, the annual forest area burned has increased by more than 1,000% relative to the mid-1980s western US (Juang et al., 2022; Reilly et al., 2022). This is not unique to the western US; Canada shattered previous burned area records in 2023 with over 18 million ha burned, 8 times the average area burned of the previous 10 years (<https://ciffc.net/situation/2023-10-06>), and Australia saw 21% of its total temperate forest biome burn in a single season (2019–2020) (Boer et al., 2020; Collins et al., 2022), nearly half of which burned at high severity (Collins et al., 2021). Given the substantial impacts on boreal and temperate forest carbon, comprehensive wall-to-wall baselines of carbon storage, drivers, and trends are vital for understanding the changing nature of the forest carbon balance.

Global estimates of forest carbon and its drivers are rapidly improving, but are often limited by inconsistencies in reporting and limited data availability (Harris et al., 2021). Further, global estimates are often produced at a coarse spatial resolution that misses important landscape-scale spatial heterogeneity in forest carbon, which is driven by myriad factors like local topographic variability (Zhang et al., 2019). Finally, global estimates can overlook region-specific drivers and the local ecology of carbon cycle science (Šimová & Storch, 2017). Thus, landscape to regional baselines are critical, in addition to global perspectives. It is also important that baselines include both live and dead carbon pools. Even the most severe disturbances, such as catastrophic stand-replacing fires, never emit 100% of forest carbon to the atmosphere (Miesel et al., 2018; van Leeuwen et al., 2014). Instead, most carbon is converted to dead biomass that either decomposes over time (Seibold et al., 2021) or serves as fuel in fire-prone regions (Jones et al., 2022; Miesel et al., 2018). Understanding the distributions, drivers, and trends of both live and dead carbon provide a more comprehensive picture of current carbon storage and is important for determining fuel loads and potential feedbacks to subsequent burning. Once carbon baselines are established, they can serve as

early warning signals for future studies to quickly identify changes and tipping points that inform future management.

The western US is a promising region to develop approaches for producing landscape to regional baselines of live and dead forest carbon. It is one of the most data rich areas on Earth, including a national network of standardized, consistently resurveyed forest plots (USDA Forest Service, 2019) and a multitude of national, regional, and remote sensing datasets characterizing potential drivers of forest carbon. The western US is also a hotspot for natural climate solutions, including the California compliance market for carbon offset credits, one of the largest of its kind in the world (Haya et al., 2020). Finally, future changes driven by drought, fire, and harvest are likely to be profound (Cook et al., 2020; Wu et al., 2023). Here, we leverage a suite of geospatial datasets in a machine learning framework to address the following objectives: (a) quantify the spatial distribution of live and dead forest carbon density (mg ha^{-1} , hereafter carbon) in western US forests at landscape to regional scales; (b) identify the climate, disturbance, human, and topographic drivers that underpin the current distribution of carbon in western forests; and (c) determine how western US forest carbon has changed since 2005.

2. Methods

2.1. Study Area and Ecoregion Selection

This study focused on 19 forested level-3 EPA ecoregions (Omernik & Griffith, 2014) within 11 Western US states: Arizona, California, Colorado, Idaho, Montana, New Mexico, Nevada, Oregon, Utah, Washington, and Wyoming. All ecoregions selected were at least 30% forested. We grouped these 19 ecoregions into five larger regions that represent shared climatic and social-ecological conditions: Pacific Northwest (PNW), Upper Rockies, Lower Rockies, Southwest (SW), and California (Figure 1). In total, our study area encompasses approximately 84% of the forested area in the western US. These forests span a vast climatic and topographic gradient and ecosystem types, from the productive temperate rainforests of the PNW to the arid woodlands of the SW.

We used the National Land Cover Database 2016 Tree Canopy Cover (NLCD 2016 TCC) layer to select forested ecoregions (Yang et al., 2018). The NLCD TCC provides percent TCC estimates of 30-m resolution grid cells based on Landsat pixels (Yang et al., 2018). We defined forested 30-m grid cells as those with at least 10% TCC and identified the percent forest cover for each ecoregion by calculating the percent of forested 30-m grid cells located within the ecoregion.

To define our forested study area within selected ecoregions, we aggregated the NLCD 2016 TCC layer to the 4-km spatial resolution of the Parameter-elevation Regressions on Independent Slopes Model (PRISM) grid using the spatially-weighted average of all contributing grid cells. We defined grid cells as forested if the aggregated TCC was greater than 10%. We selected this threshold to help eliminate noise from the “fuzz and swap” Forest Inventory and Analysis (FIA) protocol, under which plot locations are not exact. Aggregating forested area to a 4 km grid and including all grid cells with a TCC greater than 10% increased the likelihood that we still captured FIA plots with true plot locations within forested areas that were fuzzed such that they appear to be located outside forested areas. We also used the forest condition status code in the FIA database (Burrill, 2021) to select the FIA plots located within forested areas, and removed plots that did not contain at least one forested condition within the plot.

2.2. Methods Overview

We first introduce the datasets used to characterize carbon density and its potential drivers. As the carbon-driver datasets varied in spatial and temporal resolution, we describe the processing steps taken to standardize, aggregate, and synthesize them. We detail these steps by driver category in subsequent sections.

Then, we break the analysis into three conceptual parts relating to each of our three objectives. The first section is an empirical calculation of carbon measured from field surveys across the western US to establish a baseline of the current distributions of forest carbon across forested ecoregions. In the second section, we apply a data-driven machine learning approach to infer the major drivers of current carbon and their relationships with carbon within each ecoregion. The major drivers of current carbon are grouped into four categories: climate, natural disturbance, human activities, and topography. The third section identifies the empirical trends in carbon within each

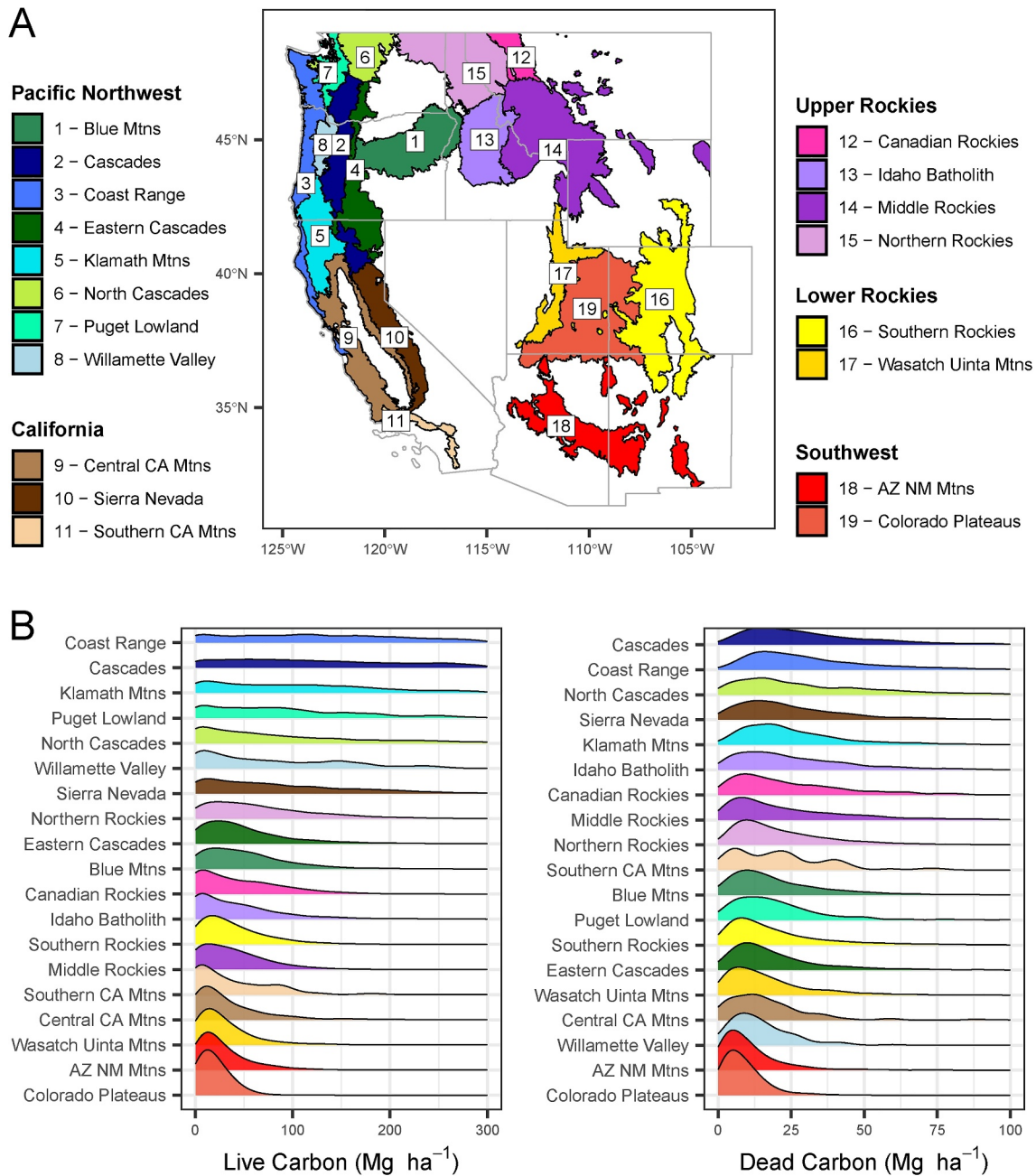


Figure 1. Map of ecoregions selected within the western US study region (a) and ecoregion distributions of live and dead carbon (b). Each of the 19 forested level-3 EPA ecoregions shown in a different color. Ecoregion colors in panel (a) match those in panels (b) and (c) and are grouped by region: PNW; blues and greens, Upper Rockies; purples, Lower Rockies; grey/yellows, SW; reds, California; browns. Ecoregion colors in panel (a) and (b) match those shown on the study region map to the right. Ecoregions in panel (b) are ordered by mean carbon within each pool, with the highest carbon values on top. Note that the x-axis in both panels has been truncated to facilitate visualization.

ecoregion since standardized field surveys began. We apply a statistical method to identify trends in carbon from 2005 to 2019.

2.3. Data Sets

Our live and dead carbon data, both current and over time, are taken from the US Forest Service FIA database (USDA Forest Service, 2019), based on forest surveys performed from 2005 to 2019. The FIA is a US national network of permanent field survey plots designed to provide continuous and standardized estimates of forest

condition. A proportion of plots in each state are measured every year, and plots are revisited every 10 years in the western US. For an in depth description of plot design see Burrill (2021). FIA provides detailed information on forest attributes, but to protect landowner privacy and ensure that landowners cannot be linked to forest data, FIA uses a “fuzz and swap” protocol. Plot coordinates are approximate but generally within 1 mile of the actual location (fuzzing), and up to 20% of FIA plots on private land are swapped with similar private plots within the same county (swapping). We chose the period 2005–2019 because 2005 is the first year where all western US states were sampled regularly (excluding Wyoming, where surveys began in 2011 and have not been re-measured) and 2019 was the most recent year available at the time of analysis. We delineated separate FIA plots using the standard “pltID” code generated by the “rFIA” package (Stanke et al., 2020), which are unique values based on a combination of the unit code, state, county, and plot values from the FIA plot table attributes (Burrill, 2021). FIA plots were selected using three criteria: (a) the reported FIA plot locations had to be in forested 4 km grid cells; (b) the FIA plots had to be classified as forested within the FIA database using the condition status code (i.e., had to have at least one forested condition within the plot) (Burrill, 2021); (c) the FIA plots had to be located within forested ecoregions selected using methods described above. We also applied an additional filter to select plots for our estimates of dead carbon. As a small portion (10%) of FIA plots did not measure downed woody material, including litter and coarse woody debris, we selected only FIA plots containing information for snags as well as downed woody material. In total, our analyses included 37,519 and 31,754 plots for the live and dead carbon analysis, respectively.

Live forest carbon was defined as above and belowground carbon density (Mg ha^{-1}) for all living trees. Trees above 1 inch (2.54 cm) diameter at 4.5 ft (1.35 m, DBH) and leaning less than 45° were included (Stanke et al., 2020). Live carbon for each plot was considered the total of foliage, tops and limbs, merchantable bole, stump, coarse roots, sapling, and woodland species, calculated using the component ratio method (Woodall et al., 2011). We defined dead carbon as the sum of the carbon density for above and belowground snag (dead tree), coarse woody debris, and litter.

We identified a series of potential drivers that are likely to underpin patterns in current carbon within ecoregions (Table S1 in Supporting Information S1). We grouped drivers into four categories: climate, natural disturbance, human activities, and topography. Below, we describe the datasets used for each driver category.

To characterize climate, we used PRISM data (Daly & Bryant, 2013). PRISM aggregates weather data from public and private stations, performs quality control, and interpolates station data values to provide gridded climate products (Daly et al., 2008). We used 4-km spatial resolution monthly estimates of mean temperatures, precipitation totals, and mean vapor pressure deficit (VPD) from 1999 to 2018.

We characterized natural disturbance in several ways, including forest wildfire area burned, forest wildfire severity, and insect and disease outbreaks. We collected annual estimates of forest area burned from the 1-km spatial resolution Western US MTBS-Interagency wildfire dataset (Juang et al., 2022). The Western US MTBS-Interagency wildfire dataset provides a comprehensive estimate of 1985–2019 fire activity throughout our study area by combining spatial fire databases to include all forest fires larger than 1 km^2 (100 ha). Dominant plant functional type as defined by Buotte et al. (2019) was also taken from the Western US MTBS-Interagency wildfire dataset. Fire severity was determined using products developed by Parks et al. (2019) which were updated for our study extent. This method uses Landsat data to estimate the composite burn index (CBI) within the perimeters of fires larger than 4 km^2 that burned between 1985 and 2019. Finally, we collected annual National Insect and Disease Aerial Detection Survey Summary Maps (Johnson & Wittwer, 2006; USDA Forest Service, 2024). This dataset provided polygons of the area affected by insects, disease, and other disturbances from 1997, and we gathered data from 1997 to 2018, the year before the last available FIA survey data.

We defined human activities drivers as land ownership categories and years since forest harvest relative to the year of survey. We determined land ownership and forest harvest year between 2000 and 2019 from the FIA database. We also characterized the legacy of forest harvest between 1986 and 2000 using the North American Forest Dynamics Forest Loss Attribution product (Schleeweis et al., 2020). This dataset uses Landsat to determine the cause of forest cover losses for the conterminous United States at a 30-m spatial resolution. For the forested areas with detectable losses, the Forest Loss Attribution product contains the likely cause of and year of forest cover loss, organized into harvest, fire, stress, conversion, and wind.

Topography was represented by slope and by ecologically-relevant landforms (Theobald et al., 2015). Landforms categorically summarize the interactions between topography (hillslope position) and solar orientation, which can impact ecological processes like soil moisture and evapotranspiration. For more information about landform category classifications, see Supporting Information S1 and Theobald et al. (2015).

2.4. Drivers of Current Carbon Distributions

Although current carbon is the result of forest processes playing out over years to decades, we specifically asked how each driver, averaged or aggregated over the longest time period possible within the dataset used, influences current carbon. To maximize the likelihood of characterizing conditions likely to be seen within each FIA plot, we aggregated all driver values taken from non-FIA datasets to the PRISM 4-km grid. Aggregation techniques varied by driver and are listed below.

2.4.1. Climate

We calculated 20-year (1999–2018) summaries of climate indices. Indices included characterizations of average climate conditions (mean annual precipitation and temperature), as well as drought conditions (precipitation of the warmest quarter and VPD of the driest quarter). This 20-year time period contains the climate conditions seen in the decade of and approximately prior to the FIA plot surveys (Table S1 in Supporting Information S1). Annual precipitation was calculated for water year (October previous year to September current year) and all other PRISM variables were calculated for calendar year. Quarters were defined as any three consecutive months, and warmest quarters were determined for each grid cell using 20-year monthly mean temperatures. Driest quarters were determined using 20-year mean monthly VPD values, where higher VPD indicates drier conditions.

2.4.2. Disturbances

To characterize fire activity, we determined cumulative 4-km grid cell burned areas from 1985 to the year before survey for each FIA plot. We estimated total cumulative forest area burned from the Western US MTBS-Interagency wildfire dataset (Juang et al., 2022), and calculated the cumulative area burned at high severity (CBI ≥ 2.25) following Parks and Abatzoglou (2020). For this study, we extended the CBI dataset spatially to include all 19 ecoregions from 1985 to 2019, and limited CBI estimates to wildfires (e.g., prescribed fires were excluded). Cumulative forest area burned and forest area burned at high severity were aggregated using the sum of contributing pixels and were expressed as percent of the 4-km grid cell area.

We determined the spatial extent of insect outbreaks and disease from the Aerial Detection Survey (Johnson & Wittwer, 2006). We selected and aggregated all polygons containing damage causing agents relating to insects and disease and calculated the percent of each grid cell area covered by selected polygons to represent the area affected. We excluded polygons from damage causing agents that were not directly relevant to insects and disease. We also restricted our estimates of insect and disease disturbance to polygons containing severe (i.e., mortality and topkill inducing) damage types that are likely to have the greatest impacts on live forest carbon. While a metric of outbreak severity exists within the Aerial Detection Survey data, the method for recording severity changes partway through the record. To avoid potential uncertainties around the severity of outbreak, we estimated the magnitude of insect and disease outbreaks as the area affected at any time in the Aerial Detection Survey record. We calculated the extent of insect and disease disturbance as the percent grid cell area affected at any point up to and including the year of survey for each FIA plot.

2.4.3. Human Activities

Land ownership was taken from FIA condition table attributes (Burrill, 2021). Land ownership was divided into four categories: undifferentiated private, federal public, Department of Defense or Energy (DOD, DOE), and non-federal (state/local/non-federal). DOD/DOE land was separated from land owned by other federal agencies as it tends to be used for military bases and training that is dissimilar to the common use of other federal lands (Vincent et al., 2020).

To estimate years since forest harvest, we first estimated harvest year between 1986 up to the year of the FIA survey, then found the difference between the year of forest harvest and the forest survey year. We created a forest harvest year metric that combined recent and legacy harvest values. The year of recent (post-2000) harvest within

a plot was taken from FIA condition table attributes (Burrill, 2021). The FIA database records the year of up to three treatments within a single plot, ranked in order of importance. We restricted our recent estimates of harvest to the FIA plots containing “cutting” (i.e., tree removal occurring within a plot; where total area affected must be at least one acer) as the most important treatment code. The legacy of past harvest was determined from the Forest Loss Attribution product (Schleeweis et al., 2020). Year of harvest from 1986 to 2000 was aggregated to 4-km spatial resolution using the average year of harvest for contributing grid cells. We assigned a final harvest year to each FIA plot using the most recent estimate available. When present, we used the recent harvest year from the FIA database. When there was no evidence of recent harvest, we used the average legacy harvest year from the Forest Loss Attribution product within the 4-km grid cell. To reduce the chance of estimating a harvest year for an unharvested FIA plot, we enforced a rule that excluded legacy harvest grid cells where cumulative harvest area was less than 25% of the grid cell area. If there was no evidence of harvest in the known record, we set the years since harvest to 100.

2.4.4. Topography

To characterize topography, we determined the slope and dominant landform within each grid cell. We gathered slope values from the “condition” table within the FIA database (Burrill, 2021), and derived FIA plot-level slope estimates by taking the area-weighted average across conditions with populated slope values. We calculated grid cell slope values as the average slope across FIA plots within each grid cell. We characterized landforms in each 4-km spatial resolution grid cell using the mode. Landform categories include ridges, upper slopes, and lower slopes which are sub-classified as cool, warm or neutral. Cliffs, valleys, and divides are also included.

2.5. Analyses

2.5.1. Quantifying Current Carbon Distribution

To assess current carbon distributions, we analyzed the most recent survey year of our forested FIA plots. The most recent survey year varied from 2007 to 2019 and 2010 to 2019 for live and dead carbon, respectively, and 96% of the live carbon plots were sampled between 2010 and 2019. We calculated the mean and standard deviation (SD) of live and dead carbon pools for all selected FIA plots in each ecoregion to evaluate and compare the distribution of carbon within and between ecoregions.

2.5.2. Modeling the Drivers of Current Carbon Distribution

Biotic and abiotic characteristics of ecoregions display high heterogeneity across the western US, so we expected the drivers of carbon to display similar heterogeneity within and across ecoregions. We therefore built separate random forest models for the live and dead carbon pools for each ecoregion to find the drivers that underpin current carbon across western forests and evaluate the importance of individual drivers. To avoid repetition in driver values when multiple FIA plots were located in the same grid cell (this occurred for ~14% of grid cells), we averaged the carbon and numerical driver values and determined the mode for categorical driver values. Random forest model predictions are known to be robust to predictor collinearity, but importance metrics can be sensitive (Aas et al., 2021; Lundberg & Lee, 2017). We reduced collinearity between numerical drivers by selecting the driver with the most explanatory power in each highly correlated pair ($r \geq 0.7$; see Supporting Information S1 for details).

Using a 5-fold cross validation framework and a 75%–25% grid cell train-test ratio for each fold, we built final random forest models for each ecoregion containing the selected numerical drivers in addition to all categorical drivers. All models also included plant functional type and the proportion forest cover of the FIA plot. We built random forest models using the “ranger” engine through the “tidymodels” interface package in R (Kuhn & Wickham, 2020; Wright & Ziegler, 2017). Models were built with 500 trees, a maximum of 10 splits per tree, and one-third of the predictors used when searching for the best split. On each fold, we used the training data to build a random forest and determined model performance and driver importance from predictions of the test datasets. To assess overall model performance, we calculated the R^2 values for the model predictions of the testing datasets in each fold and averaged the R^2 values across all folds.

To evaluate individual driver importance, we used SHapley Additive exPlanations (SHAP) values (Lundberg & Lee, 2017) from model predictions of carbon within the test datasets. We calculated and SHAP values using the

“kernelshap” package (Mayer & Watson, 2023). SHAP values calculate the effect of a driver in making model predictions for each data point (grid cell) by comparing what a model predicts with and without the driver. SHAP values summarize within-ecoregion driver importance at the data point level, but can also be aggregated across data points to summarize the importance of each driver for an entire ecoregion. We found mean SHAP values across folds for each data point to summarize within-ecoregion driver importance and calculated driver importance across grid cells in each ecoregion by finding the mean absolute 5-fold mean SHAP values across test data points. Individual driver importance was used to identify the four most important drivers in each ecoregion (hereafter referred to as “top drivers”).

We calculated partial dependence functions to determine the relationships between the top individual drivers and carbon. As the distribution of each driver and relationships between drivers can change slightly with each subsample of the FIA plots that comprise a fold, we built a model with the full dataset for each ecoregion to ensure that across the distribution of each driver, the remaining drivers are held at the best estimated mean values. Partial dependence was calculated using the “model_profile” function in the “DALEX” package (Biecek, 2018).

We assessed the relative importance of climate, fire, human activities, and topography by grouping drivers into these categories (Table S1 in Supporting Information S1). Group importance was calculated by taking the mean absolute value of all 5-fold mean test data point SHAP values for all drivers in a group, then averaging the absolute SHAP values across points as above. We determined relative driver category importance by summing all group importance and calculated the category proportion of the total.

Insect and disease presence had positive correlations with both live and dead carbon for some ecoregions (see Supporting Information S1). This positive relationship violates our ecological understanding of the effects of insects and disease based on first principles. The positive relationship in some ecoregions likely occurs because insect outbreaks and disease are correlated with another unmeasured driver of forest carbon distributions. For instance, insects and disease may have occurred preferentially in high carbon areas, but the mortality was not severe enough to affect live carbon pools. Alternatively, this positive relationship could occur because affected areas from the Aerial Detection Survey are approximated and have high uncertainties (Cohen et al., 2016; Meddens et al., 2012). In our calculations of grouped driver importance, we removed insect and disease drivers to avoid conflating disturbance with positive effects on carbon. We also enforced a rule that the area affected by insects and disease was only included in our models if relationships aligned with known ecology of their effects for each ecoregion (Supporting Information S1).

2.5.3. Recent Trends in Forest Carbon

We estimated trends in carbon for each ecoregion using a linear regression. We assessed carbon as a function of survey year, and determined trend direction and significance using coefficients and p values, respectively. We estimated the annual mean change in carbon for each ecoregion using linear regression coefficients. We calculated change between 2005 and 2019 by multiplying the linear regression coefficient by 14 (the number of years between 2005 and 2019), and defined percent change as the estimated change across the time series relative to the ecoregion mean carbon values from the most recent survey for each plot. The most recent survey was chosen to represent the baseline over the first survey to account for the large differences in the first survey year between states. We excluded plots in Wyoming from our trends analysis as there was not a long enough period of record (the first plots were sampled in 2011). We did not calculate changes in dead carbon within four ecoregions (Southern California Mountains, Sierra Nevada, Central California Mountains, and the Klamath Mountains) as downed woody material was not collected in these regions until 2011. In total, our carbon trends analyses included 37,097 and 29,571 plots for the live and dead carbon, respectively.

2.5.4. Software

All analyses were conducted in R version 4.2.2 (R Core Team, 2023) with the “chroma” (Irisson & Aisch, 2016), “DALEX” (Biecek, 2018), “DALEXtra” (Maksymiuk et al., 2021), “kernelshap” (Mayer & Watson, 2023), “rFIA” (Stanke et al., 2020) “ranger” (Wright & Ziegler, 2017), “sf” (Pebesma, 2018), “terra” (Hijmans, 2022), “tidymodels” (Kuhn & Wickham, 2020), and “tidyverse” (Wickham et al., 2019) packages.

3. Results

3.1. Current Carbon Distributions

Ecoregions of the PNW contained the highest mean live carbon, followed by the Sierra Nevada ecoregion in California, ecoregions in the Upper Rockies, Lower Rockies and SW, respectively (Figure 1, Table S2 in Supporting Information S1). Specifically, the Coast Range ecoregion in the PNW contained the highest live carbon with a mean of 174.94 (sd = 146.46) Mg ha⁻¹, while the Colorado Plateaus in the SW had the lowest (mean = 18.61, sd = 14.96 Mg ha⁻¹).

Ecoregions with the highest or lowest mean live carbon also generally had the high or low mean dead carbon. Mountainous coastal ecoregions west of the Pacific crest in the PNW contained the highest mean dead carbon, and the SW contained the lowest dead carbon values (Figure 1, Table S2 in Supporting Information S1). The Cascades in the PNW contained the highest dead carbon values of any ecoregion (mean = 35.06, sd = 30.52 Mg ha⁻¹), while the Colorado Plateaus had the lowest (mean = 8.48, sd = 7.40 Mg ha⁻¹). Unlike with live carbon, PNW ecoregions east of the Pacific crest (Eastern Cascades, Blue Mountains) or in coastal lowlands (e.g., Puget Lowland, Willamette Valley) had lower dead carbon than all Upper Rockies ecoregions.

3.2. Drivers of Carbon Distributions

We used grouped estimates of driver category importance to determine the most important drivers of carbon in each ecoregion surveyed. Climate included precipitation, temperature, and VPD variables, fire included area burned at high severity and total area burned variables, human activities included land ownership categories and years since harvest, and topography included dominant landform and slope. Grouped estimates of driver category importance only identified which groups were most important for carbon in each ecoregion, not the directionality of the relationship. We used partial dependence functions from common top individual drivers to identify the directionality of the relationship between these individual drivers and carbon.

Climate was the most important driver of live carbon for eight of 19 ecoregions surveyed, and the second most important driver for nearly all other ecoregions (excluding two PNW ecoregions), using grouped estimates of driver category importance. Fire was most important for six ecoregions, particularly in the Upper Rockies and PNW, and was the second most important driver category for another six. Human activities were most important in four PNW ecoregions and one Upper Rockies ecoregion and the second most important in two other PNW ecoregions (Figure 2, Supporting Information S1).

Estimates of grouped driver category importance show that climate and fire are also key drivers of dead carbon across the Western US. Climate was the most important driver of dead carbon for 12 ecoregions, and was the second most important driver category for all others ecoregions excluding one in the Upper Rockies (Figure 2, Supporting Information S1). Fire was the most important driver category in two PNW and three Upper Rockies ecoregions, and the second most important driver of dead carbon in another seven ecoregions across the Western US (Figure 2, Supporting Information S1). Human activities were the primary driver of dead carbon in one California and one Upper Rockies ecoregion, and were also the second most important for another ecoregion in the PNW.

Partial dependence plots for a selection of common top individual drivers of live carbon within each category and ecoregion are shown in Figure 3. Within the climate category, live carbon consistently increased with mean annual precipitation (Figure 3a) and generally declined with driest quarter VPD (Figure 3d). Every ecoregion had annual precipitation, driest quarter VPD, or mean annual temperature as a top individual driver (Figure 3). Fire (total or high severity) led to a decline in live carbon, particularly in the SW, Upper Rockies, and California (Figures 3b and 3e). Human activities were particularly important in the PNW ecoregions for individual drivers; ownership (Figure 3c) or harvest year (Figure 3f) were top drivers in every PNW ecoregion. Across PNW and Upper Rockies ecoregions, forests on federal lands had the highest live carbon, while forests on private lands contained the lowest. Live carbon also consistently declined with recent harvest. Insects and disease were only included as a driver in 10 ecoregion analyses, but when these drivers were present, we found that cumulative area affected by insects and disease was a top driver for both Lower Rockies ecoregions as well as one Upper Rockies and one California ecoregion (Supporting Information S1). Partial dependence plots for the common top individual drivers of dead carbon show similar relationships to those for live carbon (Figure 4), with the exception of cumulative area affected by fire or insects leading to an increase in dead carbon (Figure 4c).

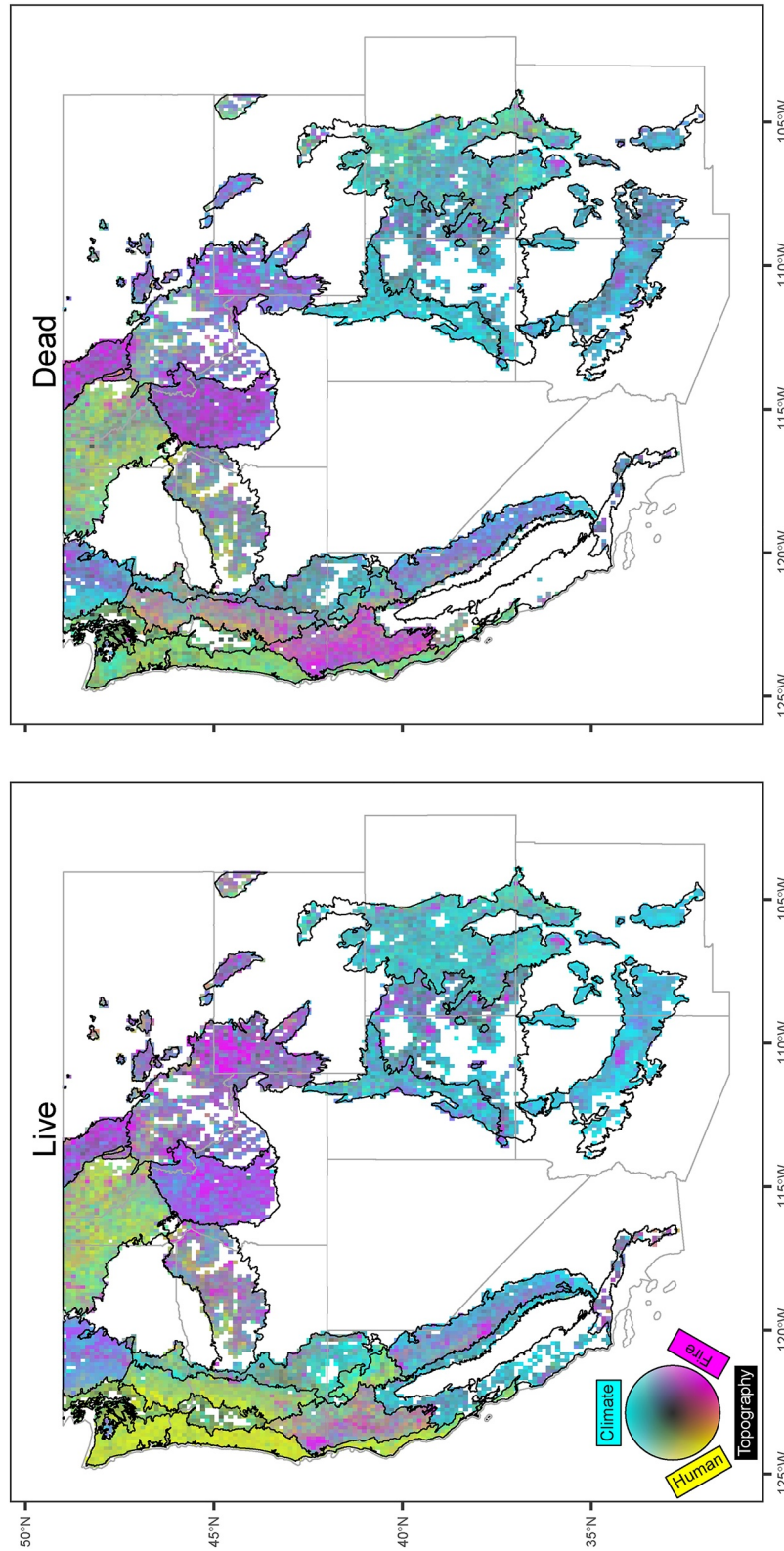


Figure 2. Relative importance of driver categories in predicting carbon densities in predicting carbon densities (climate, cyan; fire, magenta; human activities, yellow; and topography, black). Grid cells have been resampled from the original 4-km resolution to 12-km resolution to facilitate visualization.

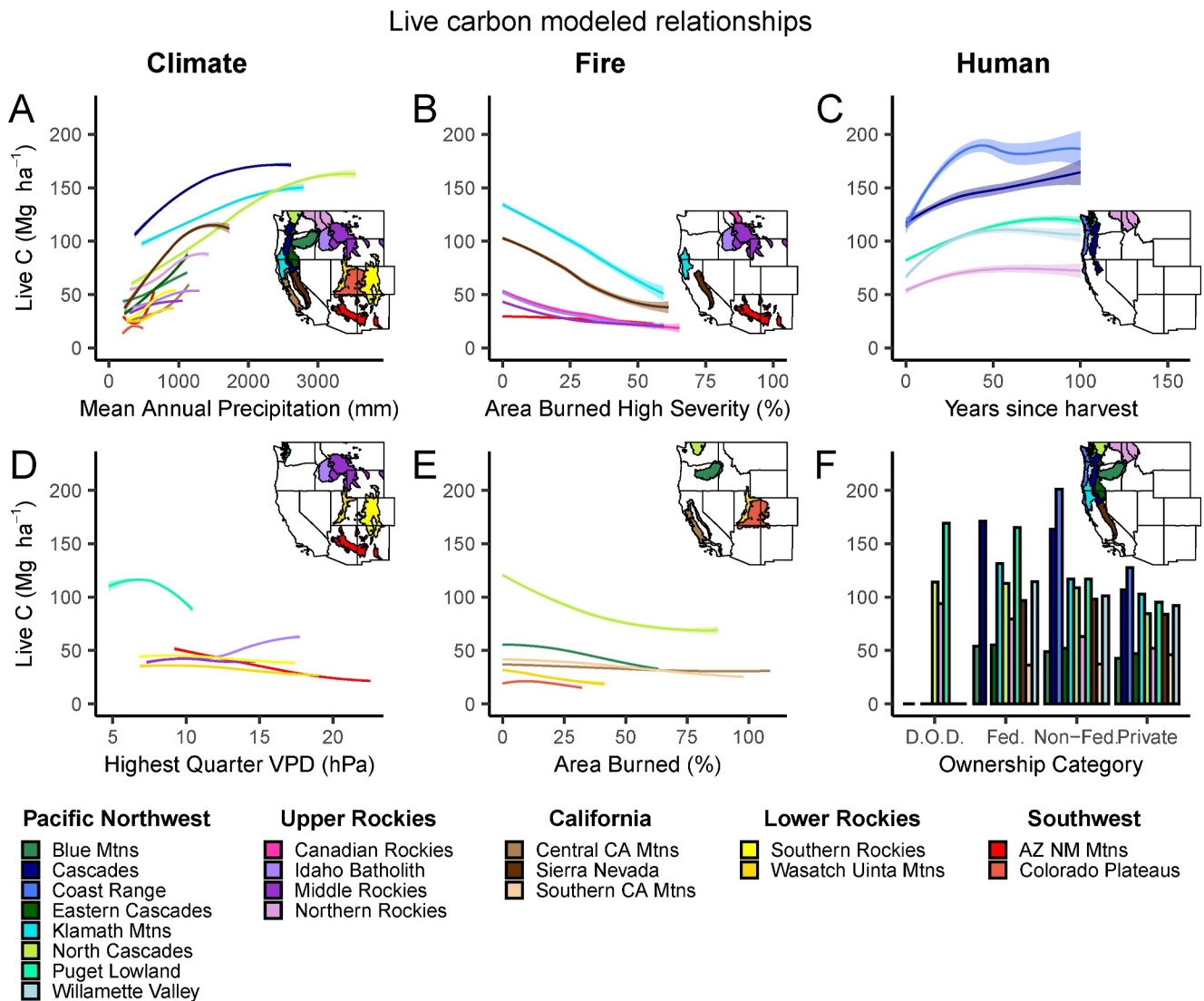


Figure 3. Relationships from partial dependence analyses between live carbon and the drivers commonly considered the top four most important. Lines represent loess (span = 1) relationships between the driver and carbon for each ecoregion where the driver was within the top four most important. Plots of continuous drivers (excluding harvest year) show the first through the 95th percentiles of each driver distribution to avoid high uncertainties at the end of the driver ranges. Plots of categorical drivers show the predicted carbon for each unique driver value.

Using 5-fold average R^2 values, random forest models accounted for 16%–42% of the variance explained in live carbon, with the Middle Rockies and North Cascades ecoregions performing worst and best, respectively. Variance explained from random forest models predicting dead carbon ranged from 2% in the Southern California Mountains to 33% in the Southern Rockies.

3.3. Recent Trends in Carbon Densities

Live carbon declined in four (21%), increased in five (26%), and remained unchanged in ten (53%) of the 19 ecoregions between 2005 and 2019 (Figure 5). Dead carbon increased in five of 15 ecoregions (33%), decreased in one (7%), and did not change in nine ecoregions (60%).

Live carbon declined in two Upper Rockies ecoregions as well as one ecoregion each in the Lower Rockies and SW (Figure 5). The most live carbon was lost in the Southern Rockies, with declines from 2005 to 2019 of $9.58 \pm 4.07 \text{ Mg ha}^{-1}$ (25%). In contrast, live carbon increased in most of the PNW ecoregions, as well as one Upper Rockies ecoregion. The Willamette Valley increased most ($39.73 \pm 31.46 \text{ Mg ha}^{-1}$, 41%), but the

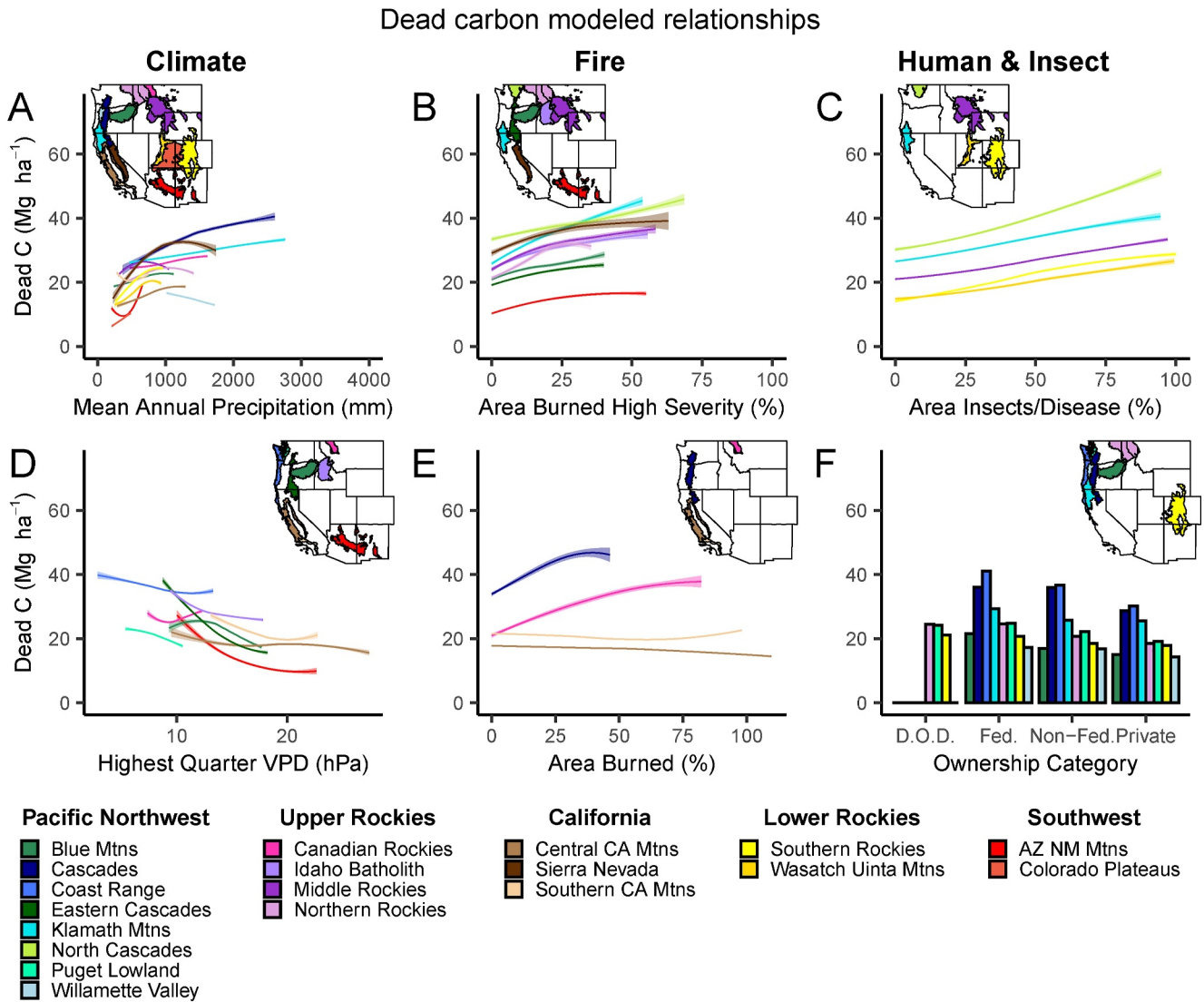


Figure 4. Relationships from partial dependence analyses between dead carbon and the drivers commonly considered the top four most important. Lines represent loess (span = 1) relationships between the driver and carbon for each ecoregion where the driver was within the top four most important. Plots of continuous drivers show the first through the 95th percentiles of each driver distribution to avoid high uncertainties at the end of the driver ranges. Plots of categorical drivers show the predicted carbon for each unique driver value.

estimates were highly uncertain due to low sample size (Figure 5). The ecoregion with the second largest live carbon increase was the Coast Range (27.28 ± 14.29 , 16%).

Dead carbon declined in one PNW ecoregion, the Coast Range (Figure 5), with a 2005 to 2019 decline in dead carbon of $-5.35 \pm 4.80 \text{ Mg ha}^{-1}$ (15%). Dead carbon increased in five ecoregions across the Western US. The ecoregion with the greatest increase in dead carbon was the Willamette Valley ($10.61 \pm 8.72 \text{ Mg ha}^{-1}$, 70%). Of the ecoregions experiencing declines in live carbon, three in the Upper and Lower Rockies also experienced increases in dead carbon.

4. Discussion

In this study, we integrated multiple external datasets with FIA plots to provide a synthetic and comprehensive perspective on western US forest carbon across landscape to ecoregion scales. We found that live forest carbon has declined across much of the western US during our study period, resulting in increased dead carbon vulnerable to release to the atmosphere through decomposition or combustion by fire. Underlying drivers of forest

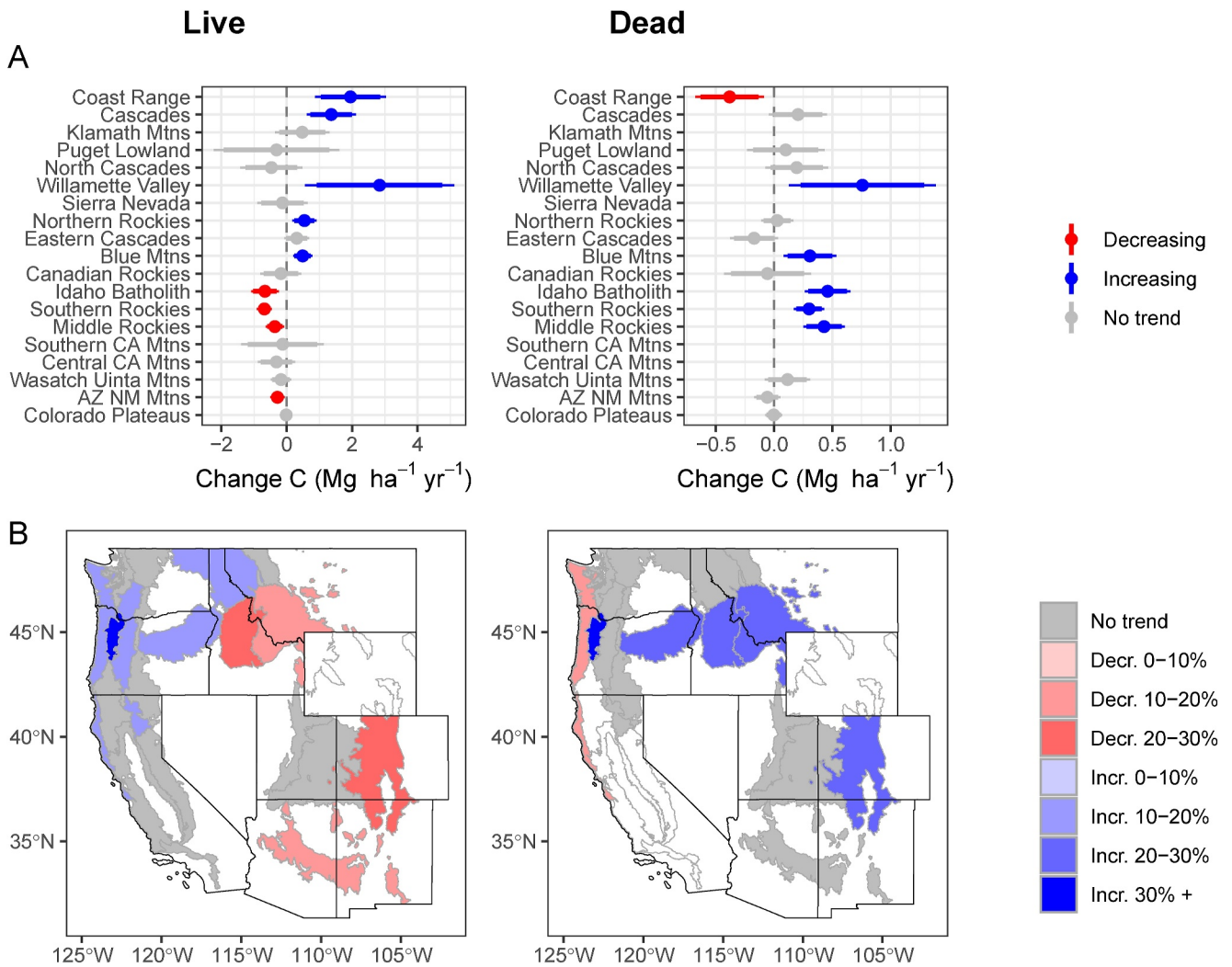


Figure 5. Estimated annual (a) and relative (b) changes in live (left) and dead (right) carbon across the time series for each ecoregion. Annual change (a) is represented by linear model coefficients and point colors represent the direction of significant trends. Relative change across the time series (b) is expressed as the percent change across the time series relative to the ecoregion mean live (bottom left) and dead (bottom right) carbon density (Mg ha^{-1}) from the most recent survey for each plot. Ecoregions in top row are ordered by mean live carbon. Forest inventory and analysis plots located in Wyoming were not included. Changes in dead carbon were not calculated for four ecoregions (Southern California Mountains, Sierra Nevada, Central California Mountains, and the Klamath Mountains) as downed woody material was not collected in these regions until 2011.

carbon exhibited strong regional patterns as well as fine-scale variability. As climate warms, disturbance regimes intensify, and intensive commercial harvest persists, our results suggest that imminent thresholds in accelerating carbon loss may be approaching. Together, these results provide key insights into the function and potential future vulnerabilities of the western US forest carbon cycle.

A number of past studies have also used FIA survey data at tree, plot, US state- and nation-wide levels to quantify western US forest carbon (Domke et al., 2023; EPA, 2023; Hoover & Smith, 2023; Knott et al., 2023; Stanke et al., 2021). However, we offer three critical advances. First, we quantify variation in carbon, underlying drivers, and recent trends within and across level III ecoregions; a scale that reflects shared geographical characteristics such as geology, land use, and potential vegetation (Omernik & Griffith, 2014). Second, we took advantage of innovations in interpretable machine learning to produce a novel framework for assessing grouped and individual driver effects on carbon, providing critical insights for informing policy and management. Finally, we leveraged external datasets to extend the record of prior disturbance and harvest back decades before FIA surveys were conducted. This allowed us to quantify the unique ecological legacies shaping current spatial distributions and recent trends in forest carbon (Johnstone et al., 2016; Seidl & Turner, 2022).

Our findings provide a baseline of forest carbon in live and dead pools across forested ecoregions in the western US. We assessed carbon by level III ecoregion in order to evaluate distributions, drivers, and trends across scales relevant to ecological processes. Despite choosing ecoregion as our scale of analysis rather than state, region, or nation, our findings generally converge with those of other FIA-based estimates of forest carbon in the western US. Hoover and Smith (2021) also found the highest aboveground live carbon densities in the PNW and the lowest in the Lower Rockies and SW. Carbon trends found in our analysis mirror regional carbon trend estimates from other FIA-based studies, such as stock changes within the National Forest System reported in the US GHG inventory (Domke et al., 2023; EPA, 2023) and live aboveground carbon changes reported within resurveyed FIA plots (Hoover & Smith, 2021).

Ecological legacies shape the spatial patterns and temporal trends of contemporary ecosystem characteristics (Johnstone et al., 2016). If disturbance legacies are not taken into account, crucial information that often determines post-disturbance reorganization outcomes can be missed (Seidl & Turner, 2022). By using external disturbance datasets collected at the landscape scale, this study extends the temporal record of disturbance data decades beyond that of the FIA plots, providing a more comprehensive understanding of landscape dynamics. We found general agreement between the FIA disturbance codes and the external fire and harvest datasets used for this analysis (Supporting Information S1). Our grid cell estimates rarely attributed high cumulative area burned to unburned FIA plots or a harvest year to unharvested FIA plots. However, there was less congruence with external insect and disease products. Grid cell estimates of area affected by insects and disease were high for many FIA plots without related FIA disturbance codes (up to approx. 70%). This suggests either that the Aerial Detection Survey (Johnson & Wittwer, 2006) affected polygons may provide an overestimation of the total area affected within grid cells, or FIA crews are missing insect-related damage in sparse forests, which may explain our counterintuitive results in how live carbon varied in response to insects and disease.

Our results indicate that climate and fire are important determinants of carbon densities within and across western US forests, particularly in ecoregions where live carbon is declining. Although annual carbon reductions through 2019 were modest, predicted increases in drought, burned area, and fire severity (Abatzoglou et al., 2021; Dennison et al., 2014; Jia, 2020; Parks & Abatzoglou, 2020; Wu et al., 2023) could foreshadow rapid acceleration of carbon loss in coming years to decades. Notably, our estimates of carbon trends also did not include Wyoming FIA plots, where we found fire and climate to be the strongest drivers of current carbon densities. This suggests we may be underestimating rates of live carbon decline in ecoregions that include forests in Wyoming (Southern Rockies, Middle Rockies).

Anthropogenic warming has already contributed to drought intensification in the western US (Crockett & Westerling, 2018), and almost all global climate models indicate drying trends will intensify, with increases in VPD and precipitation variability (Cook et al., 2021; Seager et al., 2007). Regional projections suggest that extreme drought risk could more than triple by 2100 (Cook et al., 2020). Often, precipitation and VPD were the most important drivers of carbon density in our analyses. Drought causes tree mortality (i.e., more dead carbon) through embolism and carbon starvation, and persistent drought exerts powerful selective pressures toward populations and communities with more drought-tolerant traits (Trugman et al., 2020). Further, hot-dry conditions can constrain post-disturbance tree regeneration, which also reduces forest carbon storage (Davis et al., 2023; Hansen & Turner, 2019). For example, approximately 20% of forests in the Sierra Nevada Mountains of California are anticipated to not recover if they were to burn because the climate is now too dry to support tree regeneration (Hill et al., 2023). Drying trends directly impact forests through reduced growth and increased mortality, but they also increase the occurrence of climate sensitive disturbances like fire (Jones et al., 2022).

Our analyses revealed a consistently negative relationship between live carbon and both total and stand-replacing forest area burned. Fire was either the first or second most important driver category for predicting live or dead carbon densities in two thirds of the ecoregions surveyed. No ecoregion was unaffected by fire; even PNW ecoregions with relatively infrequent fire historically contained hotspots where fire was the dominant driver category. This is likely due to fires being characteristically large and severe when they occur (Halofsky et al., 2020). As fire activity has rapidly increased (Jones et al., 2022; Juang et al., 2022), our results highlight the important role burning plays in shaping carbon across the western US. In fact, we may actually be underestimating fire effects because we excluded prescribed fires, which make up a surprisingly large percentage of annual area burned (20.6% of MTBS forest fires in 2019) (Domke et al., 2023). Further, our results did not include 2020 and 2021, exceptionally dry years toward the end of a megadrought (Williams et al., 2022) with record shattering

annual areas burned in western forests (Higuera & Abatzoglou, 2021). Wildfire in these two years alone led to the loss of 13%–19% of the total population of highly fire-adapted giant sequoias in California (Shive et al., 2022). Following 2020 and 2021, it is plausible that several additional ecoregions have already crossed critical fire and climate-driven tipping points initiating live carbon decline.

Although fire is already an important component of the carbon cycle in the western US, the impact will likely only grow over time with staggering projected increases in annual forest area burned (Abatzoglou et al., 2021; Buotte et al., 2019; Parks & Abatzoglou, 2020). Models suggest that record breaking fire seasons in 2020 and 2021 may become the norm in just a few decades (Abatzoglou et al., 2021). It is also important to note that a century of fire suppression has led to substantially higher live and dead carbon densities today than likely occurred under pre-Euro American settlement fire regimes in many dry western US forests, where fire return intervals were 5–20 years (Swetnam et al., 2016). As a result, the baseline we quantify here is critical for comparing to future conditions, but it is almost certainly inflated compared to carbon carrying capacities under the historical range of variability (Earles et al., 2014; Goodwin et al., 2020). Thus, dry forests in the western US may be acutely vulnerable to carbon loss without strong and immediate investment in proactive forest management. Targeted forest management activities such as thinning and prescribed burning have shown potential to stabilize carbon in these types of systems (Krofcheck et al., 2018, 2019). Even with forest densification from a century of suppression, however, carbon densities in dry western US forests are far lower than in historically wet cold forests where legacies of suppression are much less pronounced, and forest management may have little effect on subsequent fire (Stephens et al., 2013). For example, forests in the PNW and parts of California have some of the highest aboveground carbon densities outside of the tropics (Spawn et al., 2020). Burned area has increased rapidly in these forest types (Westerling, 2016), and given the high carbon densities at risk, they could become massive carbon sources if future climate-fire trends continue unabated.

Human activities also had a large impact on western US forest carbon. Ownership category was important for both live and dead carbon across the western US. Carbon tended to be lowest on private lands and highest on federal lands. Reduced stocks of dead carbon on private land is most pronounced in the UR, LR, and PNW ecoregions, which could be reflective of the widespread practice of removing timber affected by insects and disease to improve property values or reduce tree-fall and wildfire hazards (Morris et al., 2017). Differences in forest carbon between private and public lands were most pronounced in the PNW, where we also found clear evidence of a harvest legacy that reduced live carbon stocks relative to unharvested areas. Forests in the PNW are extraordinarily productive, commonly stocked with economically important tree species (e.g., Douglas-fir), and have a history of intensive industrial harvest (Oswalt et al., 2019; Schleeuwis et al., 2020). Our analysis revealed that PNW ecoregions generally experienced an increase in carbon densities from 2005 to 2019, which is likely representative of post-harvest regrowth (Liu et al., 2020). This regrowth could partially be attributed to the success of the Northwest Forest Plan (Spies et al., 2019), adopted in 1994 to curb removals on federally-owned old-growth forests in favor of protecting habitat for northern spotted owl populations and protecting provision of ecosystem services. On these federally-owned lands, it is likely that carbon increases would be less affected by harvest in the future than historically. However, recent carbon accumulation might also be attributable to regeneration occurring on previously harvested plantations that remain active and are simply between harvest cycles, which would not represent a permanent increase.

We also found that insects and disease were important drivers of dead carbon in many regions including the Rocky Mountains and PNW which were affected by recent bark beetle outbreaks (Bentz et al., 2005; Berner et al., 2017). Between 1997 and 2010, much of the Rocky Mountains and PNW were affected by outbreaks of mountain pine beetle, western pine beetle, spruce beetle, and Douglas-fir beetle, which led to lasting reductions in live carbon storage and sequestration (Ghimire et al., 2015). This suggests insects and disease are a major driver of carbon dynamics in the region, particularly through tree mortality and the transfer of carbon from live to dead pools. Given projected increases in forest risk from pests (Anderegg, Chegwiddden, et al., 2022), insects and disease will likely continue to play an important role in forest carbon cycling over the next century.

While tremendous differences in the distribution, drivers, and trends of carbon existed across ecoregions, there was also strong spatial variability in the primary drivers of current carbon densities within ecoregions, particularly at fine scales. For example, in the PNW, orographic effects on precipitation (Mass et al., 2022) appear to be stark and manifest in abrupt changes in the relative importance of driver categories. Within the Cascades, live carbon on the wetter and more productive western portion of the Cascades were driven primarily by human activities, while

carbon in the drier eastern portion of the Cascades was climate-dominated (Daly & Bryant, 2013). In the Klamath Mountains, carbon was driven by a mix of human, fire, and climate in the northern portion of the ecoregion, but became dominated by fire in the drier areas further south. The scale and nature of spatial heterogeneity in the drivers of carbon becomes significant when considering the scales at which management and natural climate solutions are implemented. It is critical for natural climate solutions to be considered across large regions to maximize impact and increase the rigor of measurement practices (DeFries et al., 2022), but heterogeneity in local conditions might hinder climate change mitigation efforts if the drivers of carbon vary widely within and across projects (Novick et al., 2022). Our results determining fine-scale heterogeneity in carbon drivers can therefore inform forest and fire management strategies by helping decision-makers tailor strategies to local conditions.

This study provides valuable insights into the spatial distribution and key drivers of forest carbon in western US forests. Our findings emphasize the critical role of climate, fire, and human activities in shaping forest carbon, and the strong regional patterns in dominant drivers we found underscores the need for landscape to region-specific strategies to manage carbon. The implications of our results also extend beyond understanding the current state of forest carbon in the western US. With accelerating climate changes, increasing frequency and severity of wildfires, the spread of insect and disease outbreaks, and ongoing land-use changes, western US forests face significant challenges that could result in precipitous declines in future carbon storage capacity. These challenges have the potential to fundamentally alter the terrestrial carbon cycle and undermine global efforts to combat climate change. Our results provide a baseline from which to evaluate future changes and inform management strategies.

Data Availability Statement

All data used for this analysis was taken from open-source datasets. These include forest survey data from FIA (USDA Forest Service, 2019), monthly 4 km resolution climate data from PRISM (Daly & Bryant, 2013), ADS Insect and Disease Surveys (Johnson & Wittwer, 2006; USDA Forest Service, 2024), gridded annual burned area layers from WUMI (Juang et al., 2022), fire severity estimates calculated using publicly available code provided by Parks et al. (2019), Landforms (Theobald et al., 2015), 2016 tree canopy cover maps (Yang et al., 2018), and forest cover loss attribution layers (Schleeweis et al., 2020). Analysis scripts were written using R open source software (R Core Team, 2023). Scripts are archived at the Cary Institute of Ecosystem Studies data repository (Hall et al., 2024).

References

- Aas, K., Jullum, M., & Løland, A. (2021). Explaining individual predictions when features are dependent: More accurate approximations to Shapley values. *Artificial Intelligence*, 298, 103502. <https://doi.org/10.1016/j.artint.2021.103502>
- Abatzoglou, J. T., Battisti, D. S., Williams, A. P., Hansen, W. D., Harvey, B. J., & Kolden, C. A. (2021). Projected increases in western US forest fire despite growing fuel constraints. *Communications Earth & Environment*, 2(1), 227. Article 1. <https://doi.org/10.1038/s43247-021-00299-0>
- Anderegg, W. R. L., Chegwidden, O. S., Badgley, G., Trugman, A. T., Cullenward, D., Abatzoglou, J. T., et al. (2022). Future climate risks from stress, insects and fire across US forests. *Ecology Letters*, 25(6), 1510–1520. <https://doi.org/10.1111/ele.14018>
- Anderegg, W. R. L., Trugman, A. T., Badgley, G., Anderson, C. M., Bartuska, A., Ciais, P., et al. (2020). Climate-driven risks to the climate mitigation potential of forests. *Science*, 368(6497). <https://doi.org/10.1126/science.aaz7005>
- Anderegg, W. R. L., Wu, C., Acil, N., Carvalhais, N., Pugh, T. A. M., Sadler, J. P., & Seidl, R. (2022). A climate risk analysis of Earth's forests in the 21st century. *Science*, 377(6610), 1099–1103. <https://doi.org/10.1126/science.abp9723>
- Badgley, G., Freeman, J., Hamman, J. J., Haya, B., Trugman, A. T., Anderegg, W. R. L., & Cullenward, D. (2022). Systematic over-crediting in California's forest carbon offsets program. *Global Change Biology*, 28(4), 1433–1445. <https://doi.org/10.1111/gcb.15943>
- Bentz, B., Logan, J., MacMahon, J. A., Allen, C. D., Ayres, M., Berg, E. E., et al. (2005). Bark beetle outbreaks in western North America: Causes and consequences. *Bark Beetle Symposium*. <https://pubs.er.usgs.gov/publication/70156570>
- Berner, L. T., Law, B. E., Meddens, A. J. H., & Hicke, J. A. (2017). Tree mortality from fires, bark beetles, and timber harvest during a hot and dry decade in the western United States (2003–2012). *Environmental Research Letters*, 12(6), 065005. <https://doi.org/10.1088/1748-9326/aa6f94>
- Biecek, P. (2018). DALEX: Explainers for complex predictive models in R. *Journal of Machine Learning Research*, 19(84), 1–5.
- Boer, M. M., Resco de Dios, V., & Bradstock, R. A. (2020). Unprecedented burn area of Australian mega forest fires. *Nature Climate Change*, 10(3), 171–172. Article 3. <https://doi.org/10.1038/s41558-020-0716-1>
- Buotte, P. C., Levis, S., Law, B. E., Hudiburg, T. W., Rupp, D. E., & Kent, J. J. (2019). Near-future forest vulnerability to drought and fire varies across the western United States. *Global Change Biology*, 25(1), 290–303. <https://doi.org/10.1111/gcb.14490>
- Burrill, E. A. (2021). *The forest inventory and analysis database: Database description and user guide for phase 2 (version 9.0.1)*. Database Documentation. Last modified September, 29, 2023.
- Chen, Y., Hall, J., van Wees, D., Andela, N., Hantson, S., Giglio, L., et al. (2023). Multi-decadal trends and variability in burned area from the 5th version of the global fire emissions database (GFED5). *Earth System Science Data Discussions*, 1–52. <https://doi.org/10.5194/essd-2023-182>
- Chiang, F., Mazdiyasi, O., & AghaKouchak, A. (2021). Evidence of anthropogenic impacts on global drought frequency, duration, and intensity. *Nature Communications*, 12(1), 2754. Article 1. <https://doi.org/10.1038/s41467-021-22314-w>

Acknowledgments

JH, MS, BJH, ATT, APW, and WDH acknowledge funding for this study from the Gordon and Betty Moore Foundation (GBMF11974). This paper is a contribution of the Western Fire and Forest Resilience Collaborative. JH and WDH acknowledge funding from GBMF11974 (GBMF10763), the Environmental Defense Fund, and Three Cairns Group. ATT acknowledges funding from the NSF Grants 2003205 and 2216855. APW acknowledges funding from the United States Department of Energy (DE-SC0022302). BJH acknowledges support from the Jack Corkery and George Corkery Jr. Endowed Professorship in Forest Sciences at the University of Washington. This research was supported in part by the USDA Forest Service, Rocky Mountain Research Station, Aldo Leopold Wilderness Research Institute. The findings and conclusions in this publication are those of the authors and should not be construed to represent any official USDA or US Government determination or policy.

- Cohen, W. B., Yang, Z., Stehman, S. V., Schroeder, T. A., Bell, D. M., Masek, J. G., et al. (2016). Forest disturbance across the conterminous United States from 1985–2012: The emerging dominance of forest decline. *Forest Ecology and Management*, *360*, 242–252. <https://doi.org/10.1016/j.foreco.2015.10.042>
- Collins, L., Bradstock, R. A., Clarke, H., Clarke, M. F., Nolan, R. H., & Penman, T. D. (2021). The 2019/2020 mega-fires exposed Australian ecosystems to an unprecedented extent of high-severity fire. *Environmental Research Letters*, *16*(4), 044029. <https://doi.org/10.1088/1748-9326/abeb9e>
- Collins, L., Clarke, H., Clarke, M. F., McColl Gausden, S. C., Nolan, R. H., Penman, T., & Bradstock, R. (2022). Warmer and drier conditions have increased the potential for large and severe fire seasons across south-eastern Australia. *Global Ecology and Biogeography*, *31*(10), 1933–1948. <https://doi.org/10.1111/geb.13514>
- Cook, B. I., Mankin, J. S., Marvel, K., Williams, A. P., Smerdon, J. E., & Anchukaitis, K. J. (2020). Twenty-first century drought projections in the CMIP6 forcing scenarios. *Earth's Future*, *8*(6), e2019EF001461. <https://doi.org/10.1029/2019EF001461>
- Cook, B. I., Mankin, J. S., Williams, A. P., Marvel, K. D., Smerdon, J. E., & Liu, H. (2021). Uncertainties, limits, and benefits of climate change mitigation for soil moisture drought in southwestern North America. *Earth's Future*, *9*(9), e2021EF002014. <https://doi.org/10.1029/2021EF002014>
- Crockett, J. L., & Westerling, A. L. (2018). Greater temperature and precipitation extremes intensify western U.S. Droughts, wildfire severity, and Sierra Nevada tree mortality. *Journal of Climate*, *31*(1), 341–354. <https://doi.org/10.1175/JCLI-D-17-0254.1>
- Daly, C., & Bryant, K. (2013). The PRISM climate and weather system – an introduction [Dataset]. PRISM climate group 2. Retrieved from <https://prism.oregonstate.edu/recent>
- Daly, C., Halbleib, M., Smith, J. I., Gibson, W. P., Doggett, M. K., Taylor, G. H., et al. (2008). Physiographically sensitive mapping of climatological temperature and precipitation across the conterminous United States. *International Journal of Climatology*, *28*(15), 2031–2064. <https://doi.org/10.1002/joc.1688>
- Davis, K. T., Robles, M. D., Kemp, K. B., Higuera, P. E., Chapman, T., Metlen, K. L., et al. (2023). Reduced fire severity offers near-term buffer to climate-driven declines in conifer resilience across the western United States. *Proceedings of the National Academy of Sciences*, *120*(11), e2208120120. <https://doi.org/10.1073/pnas.2208120120>
- DeFries, R., Ahuja, R., Friedman, J., Gordon, D. R., Hamburg, S. P., Kerr, S., et al. (2022). Land management can contribute to net zero. *Science*, *376*(6598), 1163–1165. <https://doi.org/10.1126/science.abo0613>
- Dennison, P. E., Brewer, S. C., Arnold, J. D., & Moritz, M. A. (2014). Large wildfire trends in the western United States, 1984–2011. *Geophysical Research Letters*, *41*(8), 2928–2933. <https://doi.org/10.1002/2014GL059576>
- Domke, G. M., Walters, B. F., Giebink, C. L., Greenfield, E. J., Smith, J. E., Nichols, M. C., et al. (2023). *Greenhouse gas emissions and removals from forest land, woodlands, urban trees, and harvested wood products in the United States, 1990–2021*. U.S. Department of Agriculture Forest Service, Washington Office. Resour. Bull. WO-101. <https://doi.org/10.2737/WO-RB-101.101>
- Earles, J. M., North, M. P., & Hurteau, M. D. (2014). Wildfire and drought dynamics destabilize carbon stores of fire-suppressed forests. *Ecological Applications*, *24*(4), 732–740. <https://doi.org/10.1890/13-1860.1>
- EPA. (2023). *Chapter 6—land use, land-use change, and forestry* (pp. 1990–2021). Inventory of U.S. Greenhouse Gas Emissions and Sinks. Retrieved from <https://www.epa.gov/system/files/documents/2023-04/US-GHG-Inventory-2023-Chapter-6-Land-Use-Land-Use-Change-and-Forestry.pdf>
- Friedlingstein, P., O'Sullivan, M., Jones, M. W., Andrew, R. M., Gregor, L., Hauck, J., et al. (2022). Global carbon budget 2022. *Earth System Science Data*, *14*(11), 4811–4900. <https://doi.org/10.5194/essd-14-4811-2022>
- Ghimire, B., Williams, C. A., Collatz, G. J., Vanderhoof, M., Rogan, J., Kulakowski, D., & Masek, J. G. (2015). Large carbon release legacy from bark beetle outbreaks across Western United States. *Global Change Biology*, *21*(8), 3087–3101. <https://doi.org/10.1111/gcb.12933>
- Gifford, L. (2020). “You can't value what you can't measure”: A critical look at forest carbon accounting. *Climatic Change*, *161*(2), 291–306. <https://doi.org/10.1007/s10584-020-02653-1>
- Goodwin, M. J., North, M. P., Zald, H. S. J., & Hurteau, M. D. (2020). Changing climate reallocates the carbon debt of frequent-fire forests. *Global Change Biology*, *26*(11), 6180–6189. <https://doi.org/10.1111/gcb.15318>
- Griscom, B. W., Adams, J., Ellis, P. W., Houghton, R. A., Lomax, G., Miteva, D. A., et al. (2017). Natural climate solutions. *Proceedings of the National Academy of Sciences*, *114*(44), 11645–11650. <https://doi.org/10.1073/pnas.1710465114>
- Hall, J., Sandor, M. E., Harvey, B. J., Parks, S. A., Trugman, A. T., Williams, A. P., & Hansen, W. D. (2024). Code associated with: Hall et al. 2024 Forest carbon storage in the Western United States: Distribution, drivers, and trends [Dataset]. Cary Institute Research Repository. <https://doi.org/10.25390/caryinstitute.25761507>
- Halofsky, J. E., Peterson, D. L., & Harvey, B. J. (2020). Changing wildfire, changing forests: The effects of climate change on fire regimes and vegetation in the Pacific Northwest, USA. *Fire Ecology*, *16*(1), 4. <https://doi.org/10.1186/s42408-019-0062-8>
- Hammond, W. M., Williams, A. P., Abatzoglou, J. T., Adams, H. D., Klein, T., López, R., et al. (2022). Global field observations of tree die-off reveal hotter-drought fingerprint for Earth's forests. *Nature Communications*, *13*(1), 1761. Article 1. <https://doi.org/10.1038/s41467-022-29289-2>
- Hansen, M. C., Potapov, P. V., Moore, R., Hancher, M., Turubanova, S. A., Tyukavina, A., et al. (2013). High-resolution global maps of 21st-century forest cover change. *Science*, *342*(6160), 850–853. <https://doi.org/10.1126/science.1244693>
- Hansen, W. D., & Turner, M. G. (2019). Origins of abrupt change? Postfire subalpine conifer regeneration declines nonlinearly with warming and drying. *Ecological Monographs*, *89*(1), e01340. <https://doi.org/10.1002/ecm.1340>
- Harris, N. L., Gibbs, D. A., Baccini, A., Birdsey, R. A., de Bruin, S., Farina, M., et al. (2021). Global maps of twenty-first century forest carbon fluxes. *Nature Climate Change*, *11*(3), 234–240. Article 3. <https://doi.org/10.1038/s41558-020-00976-6>
- Haya, B., Cullenward, D., Strong, A. L., Grubert, E., Heilmayr, R., Sivas, D. A., & Wara, M. (2020). Managing uncertainty in carbon offsets: Insights from California's standardized approach. *Climate Policy*, *20*(9), 1112–1126. <https://doi.org/10.1080/14693062.2020.1781035>
- Hepburn, C., Adlen, E., Beddington, J., Carter, E. A., Fuss, S., Mac Dowell, N., et al. (2019). The technological and economic prospects for CO₂ utilization and removal. *Nature*, *575*(7781), 87–97. Article 7781. <https://doi.org/10.1038/s41586-019-1681-6>
- Higuera, P. E., & Abatzoglou, J. T. (2021). Record-setting climate enabled the extraordinary 2020 fire season in the western United States. *Global Change Biology*, *27*(1), 1–2. <https://doi.org/10.1111/gcb.15388>
- Hijmans, R. J. (2022). terra: Spatial data analysis (1.6-7). [Computer software]. <https://cran.r-project.org/web/packages/terra/index.html>
- Hill, A. P., Nolan, C. J., Hemes, K. S., Cambron, T. W., & Field, C. B. (2023). Low-elevation conifers in California's Sierra Nevada are out of equilibrium with climate. *PNAS Nexus*, *2*(2), pgad004. <https://doi.org/10.1093/pnasnexus/pgad004>
- Hoover, C. M., & Smith, J. E. (2021). Current aboveground live tree carbon stocks and annual net change in forests of conterminous United States. *Carbon Balance and Management*, *16*(1), 17. <https://doi.org/10.1186/s13021-021-00179-2>

- Hoover, C. M., & Smith, J. E. (2023). Aboveground live tree carbon stock and change in forests of conterminous United States: Influence of stand age. *Carbon Balance and Management*, 18(1), 7. <https://doi.org/10.1186/s13021-023-00227-z>
- Irissou, J.-O., & Aisch, G. (2016). chroma: Parse and manipulate colors, create perceptually correct color palettes (0.2) [R]. <https://github.com/jiho/chroma>
- Jia, G.-S. (2020). New understanding of land-climate interactions from IPCC special report on climate change and land. *Advances in Climate Change Research*, 16(1), 9. <https://doi.org/10.12006/j.issn.1673-1719.2019.216>
- Johnson, E. W., & Wittwer, D. (2006). Aerial detection surveys in the United States. In C. Aguirre-Bravo, P. J. Pellicane, D. P. Burns, & S. Draggan (Eds.), *2006. Monitoring science and technology symposium: Unifying knowledge for sustainability in the western hemisphere proceedings RMRS-P-42CD* (pp. 809–811042). U.S. Department of Agriculture, Forest Service, Rocky Mountain Research Station. Retrieved from <https://www.fs.usda.gov/research/treearch/26577>
- Johnstone, J. F., Allen, C. D., Franklin, J. F., Frelich, L. E., Harvey, B. J., Higuera, P. E., et al. (2016). Changing disturbance regimes, ecological memory, and forest resilience. *Frontiers in Ecology and the Environment*, 14(7), 369–378. <https://doi.org/10.1002/fee.1311>
- Jones, M. W., Abatzoglou, J. T., Veraverbeke, S., Andela, N., Lasslop, G., Forkel, M., et al. (2022). Global and regional trends and drivers of fire under climate change. *Reviews of Geophysics*, 60(3), e2020RG000726. <https://doi.org/10.1029/2020RG000726>
- Juang, C. S., Williams, A. P., Abatzoglou, J. T., Balch, J. K., Hurteau, M. D., & Moritz, M. A. (2022). Rapid growth of large forest fires drives the exponential response of annual forest-fire area to aridity in the western United States. *Geophysical Research Letters*, 49(5), e2021GL097131. <https://doi.org/10.1029/2021GL097131>
- Keenan, T. F., & Riley, W. J. (2018). Greening of the land surface in the world's cold regions consistent with recent warming. *Nature Climate Change*, 8(9), 825–828. Article 9. <https://doi.org/10.1038/s41558-018-0258-y>
- Knott, J. A., Liknes, G. C., Giebink, C. L., Oh, S., Domke, G. M., McRoberts, R. E., et al. (2023). Effects of outliers on remote sensing-assisted forest biomass estimation: A case study from the United States national forest inventory. *Methods in Ecology and Evolution*, 14(7), 1587–1602. <https://doi.org/10.1111/2041-210X.14084>
- Krofcheck, D. J., Hurteau, M. D., Scheller, R. M., & Loudermilk, E. L. (2018). Prioritizing forest fuels treatments based on the probability of high-severity fire restores adaptive capacity in Sierran forests. *Global Change Biology*, 24(2), 729–737. <https://doi.org/10.1111/gcb.13913>
- Krofcheck, D. J., Remy, C. c., Keyser, A. R., & Hurteau, M. d. (2019). Optimizing forest management stabilizes carbon under projected climate and wildfires. *Journal of Geophysical Research: Biogeosciences*, 124(10), 3075–3087. <https://doi.org/10.1029/2019JG005206>
- Kuhn, M., & Wickham, H. (2020). Tidymodels: A collection of packages for modeling and machine learning using tidyverse principles. <https://www.tidymodels.org/>
- Lehmann, P., Ammunét, T., Barton, M., Battisti, A., Eigenbrode, S. D., Jepsen, J. U., et al. (2020). Complex responses of global insect pests to climate warming. *Frontiers in Ecology and the Environment*, 18(3), 141–150. <https://doi.org/10.1002/fee.2160>
- Liu, J., Sleeter, B. M., Zhu, Z., Loveland, T. R., Sohl, T., Howard, S. M., et al. (2020). Critical land change information enhances the understanding of carbon balance in the United States. *Global Change Biology*, 26(7), 3920–3929. <https://doi.org/10.1111/gcb.15079>
- Lundberg, S. M., & Lee, S.-I. (2017). A unified approach to interpreting model predictions. *Advances in Neural Information Processing Systems*, 30. <https://proceedings.neurips.cc/paper/2017/hash/8a20a8621978632d76c43dfd28b67767-Abstract.html>
- Maksymiuk, S., Gosiewska, A., & Biecek, P. (2021). Landscape of R packages for eXplainable Artificial Intelligence (arXiv:2009.13248). *arXiv*. <https://doi.org/10.48550/arXiv.2009.13248>
- Mass, C. F., Salathé, E. P., Steed, R., & Baars, J. (2022). The mesoscale response to global warming over the Pacific Northwest evaluated using a regional climate model ensemble. *Journal of Climate*, 35(6), 2035–2053. <https://doi.org/10.1175/JCLI-D-21-0061.1>
- Mayer, M., & Watson, D. (2023). kernelshap: Kernel SHAP (0.3.7). [Computer software]. <https://cran.r-project.org/web/packages/kernelshap/index.html>
- Meddens, A. J. H., Hicke, J. A., & Ferguson, C. A. (2012). Spatiotemporal patterns of observed bark beetle-caused tree mortality in British Columbia and the western United States. *Ecological Applications*, 22(7), 1876–1891. <https://doi.org/10.1890/11-1785.1>
- Miesel, J., Reiner, A., Ewell, C., Maestrini, B., & Dickinson, M. (2018). Quantifying changes in total and pyrogenic carbon stocks across fire severity gradients using active wildfire incidents. *Frontiers in Earth Science*, 6. <https://doi.org/10.3389/feart.2018.00041>
- Morris, J. L., Cottrell, S., Fettig, C. J., Hansen, W. D., Sherriff, R. L., Carter, V. A., et al. (2017). Managing bark beetle impacts on ecosystems and society: Priority questions to motivate future research. *Journal of Applied Ecology*, 54(3), 750–760. <https://doi.org/10.1111/1365-2664.12782>
- Novick, K., Williams, C., Rankle, B., Anderegg, W., Hollinger, D., Litvak, M., et al. (2022). The science needed for robust, scalable, and credible nature-based climate solutions in the United States: Full report. *IUScholarWorks*. <https://doi.org/10.5967/N7R9-7J83>
- Omernik, J. M., & Griffith, G. E. (2014). Ecoregions of the conterminous United States: Evolution of a hierarchical spatial framework. *Environmental Management*, 54(6), 1249–1266. <https://doi.org/10.1007/s00267-014-0364-1>
- Oswalt, S. N., Smith, W. B., Miles, P. D., & Pugh, S. A. (2019). *Forest Resources of the United States, 2017: A technical document supporting the forest Service 2020 RPA assessment (WO-GTR-97; p. WO-GTR-97)*. U.S. Department of Agriculture, Forest Service. <https://doi.org/10.2737/WO-GTR-97>
- Parks, S. A., & Abatzoglou, J. T. (2020). Warmer and drier fire seasons contribute to increases in area burned at high severity in western US forests from 1985 to 2017. *Geophysical Research Letters*, 47(22), e2020GL089858. <https://doi.org/10.1029/2020GL089858>
- Parks, S. A., Holsinger, L. M., Koontz, M. J., Collins, L., Whitman, E., Parisien, M.-A., et al. (2019). Giving ecological meaning to satellite-derived fire severity metrics across North American forests. *Remote Sensing*, 11(14), 1735. Article 14. <https://doi.org/10.3390/rs11141735>
- Pebesma, E. (2018). Simple features for R: Standardized support for spatial vector data. *The R Journal*, 10(1), 439. <https://doi.org/10.32614/RJ-2018-009>
- Pokhrel, Y., Felfelani, F., Satoh, Y., Boulange, J., Burek, P., Gädeke, A., et al. (2021). Global terrestrial water storage and drought severity under climate change. *Nature Climate Change*, 11(3), 226–233. Article 3. <https://doi.org/10.1038/s41558-020-00972-w>
- R Core Team. (2023). R: A language and environment for statistical computing (4.2.2). [Computer software]. R Foundation for Statistical Computing. Retrieved from <https://www.R-project.org/>
- Reilly, M. J., Zupan, A., Halofsky, J. S., Raymond, C., McEvoy, A., Dye, A. W., et al. (2022). Cascadia Burning: The historic, but not historically unprecedented, 2020 wildfires in the Pacific Northwest, USA. *Ecosphere*, 13(6), e4070. <https://doi.org/10.1002/ecs2.4070>
- Rockström, J., Beringer, T., Hole, D., Griscom, B., Mascia, M. B., Folke, C., & Creutzig, F. (2021). We need biosphere stewardship that protects carbon sinks and builds resilience. *Proceedings of the National Academy of Sciences*, 118(38), e2115218118. <https://doi.org/10.1073/pnas.2115218118>
- Rogelj, J., Shindell, D., Jiang, K., Fifita, S., Forster, P., Ginzburg, V., et al. (2018). Mitigation pathways compatible with 1.5°C in the context of sustainable development. In *Global warming of 1.5°C* (pp. 93–174). Intergovernmental Panel on Climate Change. Retrieved from https://www.ipcc.ch/site/assets/uploads/sites/2/2018/07/SR15_Chapter2_High_Res.pdf

- Ruehr, S., Keenan, T. F., Williams, C., Zhou, Y., Lu, X., Bastos, A., et al. (2023). Evidence and attribution of the enhanced land carbon sink. *Nature Reviews Earth and Environment*, 4(8), 518–534. Article 8. <https://doi.org/10.1038/s43017-023-00456-3>
- Schleeweis, K. G., Moisen, G. G., Schroeder, T. A., Toney, C., Freeman, E. A., Goward, S. N., et al. (2020). US national maps attributing forest change: 1986–2010 [Dataset]. *Forests*, 11(6), 653. Article 6. <https://doi.org/10.3390/f11060653>
- Seager, R., Ting, M., Held, I., Kushnir, Y., Lu, J., Vecchi, G., et al. (2007). Model projections of an imminent transition to a more arid climate in southwestern North America. *Science*, 316(5828), 1181–1184. <https://doi.org/10.1126/science.1139601>
- Seibold, S., Rammer, W., Hothorn, T., Seidl, R., Ulyshen, M. D., Lorz, J., et al. (2021). The contribution of insects to global forest deadwood decomposition. *Nature*, 597(7874), 77–81. Article 7874. <https://doi.org/10.1038/s41586-021-03740-8>
- Seidl, R., & Turner, M. G. (2022). Post-disturbance reorganization of forest ecosystems in a changing world. *Proceedings of the National Academy of Sciences*, 119(28), e2202190119. <https://doi.org/10.1073/pnas.2202190119>
- Shive, K. L., Wuenschel, A., Hardlund, L. J., Morris, S., Meyer, M. D., & Hood, S. M. (2022). Ancient trees and modern wildfires: Declining resilience to wildfire in the highly fire-adapted giant sequoia. *Forest Ecology and Management*, 511, 120110. <https://doi.org/10.1016/j.foreco.2022.120110>
- Šimová, I., & Storch, D. (2017). The enigma of terrestrial primary productivity: Measurements, models, scales and the diversity–productivity relationship. *Ecography*, 40(2), 239–252. <https://doi.org/10.1111/ecog.02482>
- Spawn, S. A., Sullivan, C. C., Lark, T. J., & Gibbs, H. K. (2020). Harmonized global maps of above and belowground biomass carbon density in the year 2010. *Scientific Data*, 7(1), 112. <https://doi.org/10.1038/s41597-020-0444-4>
- Spies, T. A., Long, J. W., Charnley, S., Hessburg, P. F., Marcot, B. G., Reeves, G. H., et al. (2019). Twenty-five years of the Northwest Forest Plan: What have we learned? *Frontiers in Ecology and the Environment*, 17(9), 511–520. <https://doi.org/10.1002/fee.2101>
- Spinoni, J., Barbosa, P., De Jager, A., McCormick, N., Naumann, G., Vogt, J. V., et al. (2019). A new global database of meteorological drought events from 1951 to 2016. *Journal of Hydrology: Regional Studies*, 22, 100593. <https://doi.org/10.1016/j.ejrh.2019.100593>
- Stanke, H., Finley, A. O., Domke, G. M., Weed, A. S., & MacFarlane, D. W. (2021). Over half of western United States' most abundant tree species in decline. *Nature Communications*, 12(1), 451. <https://doi.org/10.1038/s41467-020-20678-z>
- Stanke, H., Finley, A. O., Weed, A. S., Walters, B. F., & Domke, G. M. (2020). rFIA: An R package for estimation of forest attributes with the US Forest Inventory and Analysis database. *Environmental Modelling and Software*, 127, 104664. <https://doi.org/10.1016/j.envsoft.2020.104664>
- Stephens, S. L., Agee, J. K., Fulé, P. Z., North, M. P., Romme, W. H., Swetnam, T. W., & Turner, M. G. (2013). Managing forests and fire in changing climates. *Science*, 342(6154), 41–42. <https://doi.org/10.1126/science.1240294>
- Swetnam, T. W., Farella, J., Roos, C. I., Liebmann, M. J., Falk, D. A., & Allen, C. D. (2016). Multiscale perspectives of fire, climate and humans in western North America and the Jemez Mountains, USA. *Philosophical Transactions of the Royal Society B: Biological Sciences*, 371(1696), 20150168. <https://doi.org/10.1098/rstb.2015.0168>
- Tagesson, T., Schurgers, G., Horion, S., Ciais, P., Tian, F., Brandt, M., et al. (2020). Recent divergence in the contributions of tropical and boreal forests to the terrestrial carbon sink. *Nature Ecology & Evolution*, 4(2), 202–209. Article 2. <https://doi.org/10.1038/s41559-019-1090-0>
- Theobald, D. M., Harrison-Atlas, D., Monahan, W. B., & Albano, C. M. (2015). Ecologically-relevant maps of landforms and physiographic diversity for climate adaptation planning [Dataset]. *PLoS One*, 10(12), e0143619. <https://doi.org/10.1371/journal.pone.0143619>
- Trugman, A. T., Anderegg, L. D. L., Shaw, J. D., & Anderegg, W. R. L. (2020). Trait velocities reveal that mortality has driven widespread coordinated shifts in forest hydraulic trait composition. *Proceedings of the National Academy of Sciences*, 117(15), 8532–8538. <https://doi.org/10.1073/pnas.1917521117>
- USDA Forest Service. (2019). Forest inventory and analysis database [Dataset]. Forest Service Research Data Archive. <https://doi.org/10.2737/RDS-2001-FIADB>
- USDA Forest Service. (2024). Aerial detection surveys: Insect and disease detection survey [Dataset]. USDA Forest Service. Retrieved from <https://www.fs.usda.gov/foresthealth/applied-sciences/mapping-reporting/detection-surveys.shtml>
- van Leeuwen, T. T., van der Werf, G. R., Hoffmann, A. A., Detmers, R. G., Rucker, G., French, N. H. F., et al. (2014). Biomass burning fuel consumption rates: A field measurement database. *Biogeosciences*, 11(24), 7305–7329. <https://doi.org/10.5194/bg-11-7305-2014>
- van Wees, D., van der Werf, G. R., Randerson, J. T., Andela, N., Chen, Y., & Morton, D. C. (2021). The role of fire in global forest loss dynamics. *Global Change Biology*, 27(11), 2377–2391. <https://doi.org/10.1111/gcb.15591>
- Vincent, C. H., Bermejo, L. F., & Hanson, L. A. (2020). Federal land ownership: Overview and data.
- Walker, A. P., De Kauwe, M. G., Bastos, A., Belmecheri, S., Georgiou, K., Keeling, R. F., et al. (2021). Integrating the evidence for a terrestrial carbon sink caused by increasing atmospheric CO₂. *New Phytologist*, 229(5), 2413–2445. <https://doi.org/10.1111/nph.16866>
- Walker, W. S., Gorelik, S. R., Cook-Patton, S. C., Baccini, A., Farina, M. K., Solvik, K. K., et al. (2022). The global potential for increased storage of carbon on land. *Proceedings of the National Academy of Sciences*, 119(23), e2111312119. <https://doi.org/10.1073/pnas.2111312119>
- Westerling, A. L. (2016). Increasing western US forest wildfire activity: Sensitivity to changes in the timing of spring. *Philosophical Transactions of the Royal Society B: Biological Sciences*, 371(1696), 20150178. <https://doi.org/10.1098/rstb.2015.0178>
- Wickham, H., Averick, M., Bryan, J., Chang, W., McGowan, L. D., François, R., et al. (2019). Welcome to the tidyverse. *Journal of Open Source Software*, 4(43), 1686. <https://doi.org/10.21105/joss.01686>
- Williams, A. P., Cook, B. I., & Smerdon, J. E. (2022). Rapid intensification of the emerging southwestern North American megadrought in 2020–2021. *Nature Climate Change*, 12(3), 232–234. Article 3. <https://doi.org/10.1038/s41558-022-01290-z>
- Woodall, C. W., Heath, L. S., Domke, G. M., & Nichols, M. C. (2011). *Methods and equations for estimating aboveground volume, biomass, and carbon for trees in the U.S. forest inventory*. U.S. Department of Agriculture, Forest Service. 2010 (NRS-GTR-88; p. NRS-GTR-88). <https://doi.org/10.2737/NRS-GTR-88>
- Wright, M. N., & Ziegler, A. (2017). Ranger: A fast implementation of random forests for high dimensional data in C++ and R. *Journal of Statistical Software*, 77, 1–17. <https://doi.org/10.18637/jss.v077.i01>
- Wu, C., Coffield, S. R., Goulden, M. L., Randerson, J. T., Trugman, A. T., & Anderegg, W. R. L. (2023). Uncertainty in US forest carbon storage potential due to climate risks. *Nature Geoscience*, 16(5), 422–429. Article 5. <https://doi.org/10.1038/s41561-023-01166-7>
- Yang, H., Ciais, P., Frappart, F., Li, X., Brandt, M., Fensholt, R., et al. (2023). Global increase in biomass carbon stock dominated by growth of northern young forests over past decade. *Nature Geoscience*, 16(10), 886–892. Article 10. <https://doi.org/10.1038/s41561-023-01274-4>
- Yang, L., Jin, S., Danielson, P., Homer, C., Gass, L., Bender, S. M., et al. (2018). A new generation of the United States National Land Cover Database: Requirements, research priorities, design, and implementation strategies [Dataset]. *ISPRS Journal of Photogrammetry and Remote Sensing*, 146, 108–123. <https://doi.org/10.1016/j.isprsjprs.2018.09.006>
- Zhang, Y., Liang, S., & Yang, L. (2019). A review of regional and global gridded forest biomass datasets. *Remote Sensing*, 11(23), 2744. Article 23. <https://doi.org/10.3390/rs11232744>
- Zheng, B., Ciais, P., Chevallier, F., Chuvieco, E., Chen, Y., & Yang, H. (2021). Increasing forest fire emissions despite the decline in global burned area. *Science Advances*, 7(39), eabh2646. <https://doi.org/10.1126/sciadv.abh2646>